colorants

MDPI

Article

Synthesis and Color Evaluation of Tb^{4+}-Doped Na_2ZrO_3 for Inorganic Yellow Pigments

Ryohei Oka [1,*], Tomoyo Nouchi [2] and Toshiyuki Masui [2,*]

[1] Field of Advanced Ceramics, Department of Life Science and Applied Chemistry, Nagoya Institute of Technology, Gokiso, Showa, Nagoya 466-8555, Aichi, Japan
[2] Department of Chemistry and Biotechnology, Faculty of Engineering, Center for Research on Green Sustainable Chemistry, Tottori University, 4-101, Koyama-cho Minami, Tottori 680-8552, Tottori, Japan; b16t3062x@gmail.com
* Correspondence: oka.ryohei@nitech.ac.jp (R.O.); masui@tottori-u.ac.jp (T.M.); Tel.: +81-52-735-5365 (R.O.); +81-857-31-5264 (T.M.)

Abstract: Tb^{4+}-doped sodium zirconate samples, $Na_2Zr_{1-x}Tb_xO_3$, were synthesized as novel environmentally friendly inorganic yellow pigments by a conventional solid-state reaction method. Their crystal structures, optical properties, and colors were characterized. A single-phase form was obtained for the samples in the x range of $x \leq 0.18$, while impurity phases were detected for the sample with $x = 0.20$. All samples showed strong optical absorption in the blue light region, due to the charge transfer transition between O^{2-} and Tb^{4+}. As a result, the sample color became yellow, which is the complementary color of blue, and the color became more vivid with increasing Tb^{4+} content in the single-phase region. Among the samples, $Na_2Zr_{0.82}Tb_{0.18}O_3$ was the optimal composition, with the highest yellowness (b^* = +67.2) and pure yellow hue (h° = 90.1). Although the b^* value was lower than commercial yellow pigments such as $BiVO_4$ and $ZrSiO_4$:Pr, this sample had a purer yellow hue. Since $Na_2Zr_{0.82}Tb_{0.18}O_3$ is composed of non-toxic elements, it could be a new environmentally friendly inorganic yellow pigment.

Keywords: yellow pigment; environmentally friendly; Tb^{4+} ion; sodium zirconate

Citation: Oka, R.; Nouchi, T.; Masui, T. Synthesis and Color Evaluation of Tb^{4+}-Doped Na_2ZrO_3 for Inorganic Yellow Pigments. *Colorants* **2022**, *1*, 347–353. https://doi.org/10.3390/colorants1030020

Academic Editor: Anthony Harriman

Received: 29 June 2022
Accepted: 27 July 2022
Published: 1 August 2022

1. Introduction

Inorganic pigments have been widely applied to products such as inks, paints, ceramics, and so on. Particularly, yellow pigments are used in paints for warning signboards and traffic road markers owing to their high visibility [1]. Chrome yellow ($PbCrO_4$), cadmium yellow (CdS), and nickel–titanium yellow (TiO_2-NiO-Sb_2O_3) pigments have been used as industrial yellow pigments. However, these pigments contain elements (e.g., Pb, Cr, Cd, and Sb) that are toxic to humans and the environment. The use of these existing pigments has so far been prohibited or restricted, and there has been a need to develop novel yellow pigments. In light of this situation, a number of studies have been reported by several researchers [2–13]. However, there are few high-performance inorganic yellow pigments that are environmentally friendly, demonstrate sufficient chemical/thermal stability, and comparable to the conventional products. In addition, oxide materials that are highly stable and can be synthesized in processes that do not use toxic gases are desired to provide more sustainable and environmentally friendly materials.

In view of this situation, we focused on Tb^{4+} as a yellow coloring source and proposed a new concept in the development of yellow pigments. Some compounds such as A(Sn, Tb)O_3 (A = Sr, Ba) [14–17], A_2(B, Tb)O_4 (A = Sr, Ba; B = Zr, Sn, Ce) [18–20], and Bi_3(Y, Tb)$O_{6+\delta}$ [21] have been proposed as environmentally friendly yellow pigments. These compounds absorb visible light in the blue light region due to the charge transfer (CT) transition between O^{2-} and Tb^{4+} and exhibit a yellow color. In most cases of these materials,

the Tb^{4+} ions are introduced into the octahedral [MO_6] (M = metal) sites. Therefore, when Tb^{4+} ions are doped into [MO_6] octahedra, a yellow color will be obtained.

In this study, we selected sodium zirconate, Na_2ZrO_3, as a host material. This compound is composed of only non-toxic and cost-effective elements. A Na_2ZrO_3 structure includes octahedral [ZrO_6] sites [22–25] and the valence of Zr in this structure is tetravalent. The valence of Zr^{4+} is equivalent to Tb^{4+} and the ionic radius of Zr^{4+} (0.072 nm [26]) is close to that of Tb^{4+} (0.076 nm [26]) in size. For these reasons, we thought Tb^{4+} ions could be introduced into the octahedral Zr^{4+} site to exhibit a yellow color. Therefore, in this study, Tb^{4+}-doped Na_2ZrO_3 samples were synthesized, and their optical and color properties were characterized as environmentally friendly inorganic yellow pigments. Considering the viewpoint of practical use, the sample color was compared with commercial inorganic yellow pigments, and the chemical stability was also evaluated.

2. Materials and Methods

2.1. Synthesis

The $Na_2Zr_{1-x}Tb_xO_3$ ($0 \leq x \leq 0.20$) samples were synthesized via a solid-state reaction method. Stoichiometric amounts of ZrO_2 (FUJIFILM Wako Pure Chemical, 98.0%, Fujifilm, Tokyo, Japan) and Tb_4O_7 (FUJIFILM Wako Pure Chemical, 99.9%) and 1.6 times the stoichiometric amounts of Na_2CO_3 (Kanto Chemical, Tokyo, Japan, 99.5%) were mixed in an agate mortar for 30 min to obtain 2 g of the final product. The mixtures were calcined in an alumina crucible at 1200 °C for 5 h in air. Finally, the samples were ground in an agate mortar before characterization.

2.2. Characterization

The crystal phase and structure were identified by X-ray powder diffraction (XRD; Ultima IV, Rigaku, Tokyo, Japan). The XRD patterns were captured with Cu-Kα radiation operating at 40 kV and 40 mA. The data were collected by scanning over the 2θ range of 20–80°. The sampling width was 0.02° and the scan speed was 6° min^{-1}. The lattice volumes were calculated from the XRD peak angles refined by α-Al_2O_3 as a standard and using the CellCalc Ver. 2.20 software. The morphologies were observed by using field-emission-type scanning electron microscopy (FE-SEM; JEOL, Tokyo, Japan, JSM-6701F).

To investigate optical properties of the powder samples, the optical reflectance spectra were recorded on an ultraviolet–visible–near-infrared (UV–Vis-NIR) spectrometer (JASCO, Tokyo, Japan, V-770 with an integrating sphere attachment) using a standard white plate as a reference. The step width was 1 nm and the scan rate was 1000 nm min^{-1}. The color properties of the powder samples were evaluated in terms of the Commission Internationale de l'Éclairage (CIE) $L^*a^*b^*Ch^\circ$ system, using a colorimeter (Konica-Minolta, Tokyo, Japan, CR-300). The L^* parameter indicates the brightness or darkness in a neutral grayscale. The a^* and b^* values represent the red–green and yellow–blue axes, respectively. The chroma parameter (C) denotes the color saturation and is calculated with the formula, $C = [(a^*)^2 + (b^*)^2]^{1/2}$. The hue angle ($h^\circ$) ranges from 0 to 360° and is estimated according to the following formula: $h^\circ = \arctan(b^*/a^*)$. The standard deviations of all values for the $L^*a^*b^*Ch^\circ$ color coordinate data were less than 0.1.

3. Results and Discussion

3.1. X-ray Powder Diffraction (XRD) and Scanning Electron Microscopy (SEM)

Figure 1 shows the XRD patterns of the $Na_2Zr_{1-x}Tb_xO_3$ ($0 \leq x \leq 0.20$) samples. In the x range from 0 to 0.18, the Na_2ZrO_3 phase was obtained in a single-phase form. For x = 0.20, on the other hand, the target phase was observed as the primary phase, but additional impurity peaks indexed to ZrO_2 and $Tb_{11}O_{20}$ were also detected.

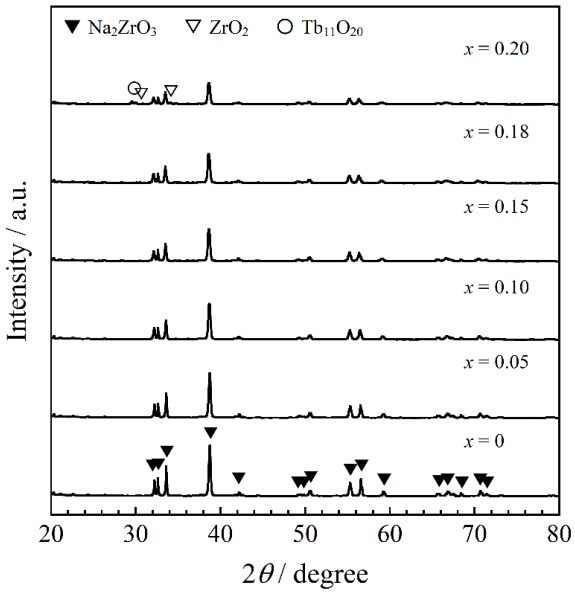

Figure 1. XRD patterns of the $Na_2Zr_{1-x}Tb_xO_3$ ($0 \leq x \leq 0.20$) samples.

The crystal structure of Na_2ZrO_3 belongs to a monoclinic system with a symmetry of the $C2/c$ (no. 15) space group. In the Na_2ZrO_3 structure, both Na^+ and Zr^{4+} coordination numbers are six and there are [NaO_6] and [ZrO_6] octahedra in the lattice [22]. The composition dependence of the lattice volume of the samples calculated from each XRD pattern is shown in Figure 2. The lattice volume was found to increase linearly with increasing Tb^{4+} content in the $x \leq 0.18$ range by introducing larger Tb^{4+} (ionic radius: 0.076 nm [26]) ions into the Zr^{4+} (ionic radius: 0.072 nm [26]) sites. The cell volume at x = 0.20 was almost equal to that at x = 0.18. Therefore, solid solutions of $Na_2Zr_{1-x}Tb_xO_3$ were successfully synthesized in the region of x = 0 to 0.18.

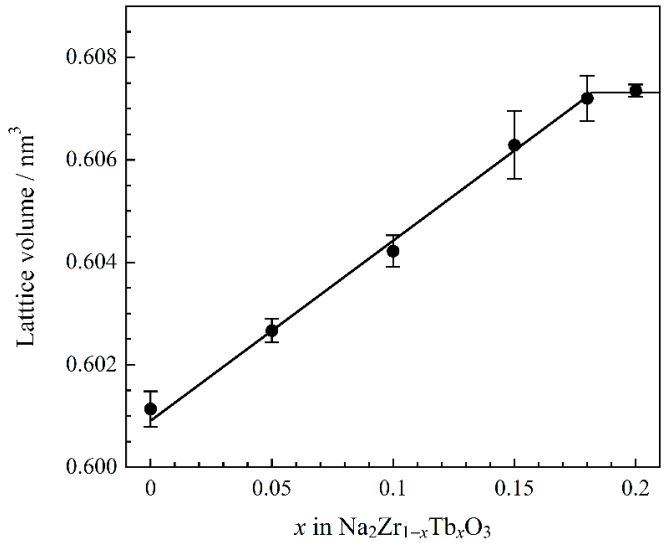

Figure 2. Compositional dependence of the lattice volume for the $Na_2Zr_{1-x}Tb_xO_3$ ($0 \leq x \leq 0.20$) samples.

Figure 3 shows the SEM images of the $Na_2Zr_{1-x}Tb_xO_3$ (x = 0 and 0.18) samples obtained in a single-phase form. The size of the primary particles in both samples was approximately 5 μm. The primary particles were thermochemically fused to form coarse secondary particles, due to the high calcination temperature of 1200 °C.

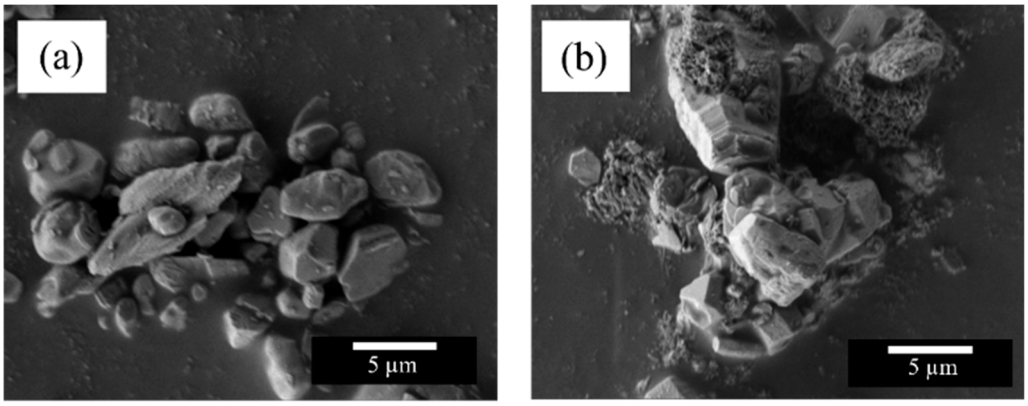

Figure 3. SEM images of the $Na_2Zr_{1-x}Tb_xO_3$ (x = 0 and 0.18) samples; (**a**) x = 0, (**b**) x = 0.18.

3.2. Ultraviolet-Visible (UV-Vis) Reflectance Spectra

The UV–Vis reflectance spectra of $Na_2Zr_{1-x}Tb_xO_3$ ($0 \leq x \leq 0.20$) are depicted in Figure 4. The host material exhibited high reflectance in the visible region and was white in color. Except for the $Na_2Zr_{0.80}Tb_{0.20}O_3$ (x = 0.20) sample, the Tb^{4+}-doped samples strongly absorbed the blue light at wavelengths between 435 and 480 nm, and this optical absorption was attributed to the charge transfer (CT) transition between O^{2-} and Tb^{4+} [17,19]. Since blue is the complementary color of yellow, these samples are yellow. On the other hand, the sample with x = 0.20 absorbed visible light in the longer wavelength region. The impurity phase, $Tb_{11}O_{20}$, detected in Figure 1 contains both Tb^{3+} and Tb^{4+}. This compound absorbs visible light through charge transfer transitions between metal ions with different valence [27]. On the other hand, the other impurity, ZrO_2, is white in color and generally shows no optical absorption in the visible light region. Therefore, the additional optical absorption observed in the sample with x = 0.20 was attributed to charge transfer transitions between Tb^{3+} and Tb^{4+}.

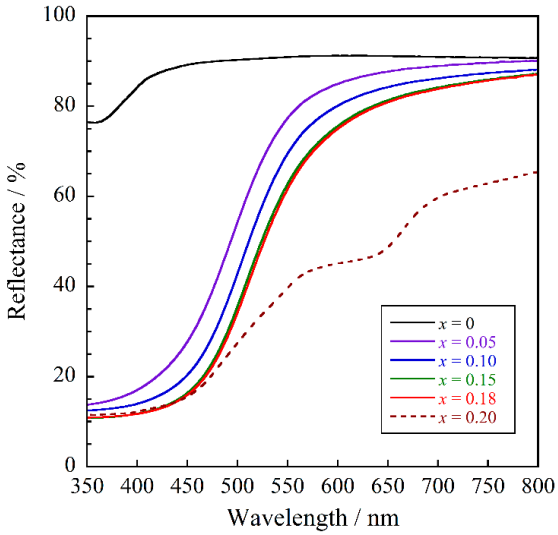

Figure 4. UV–Vis reflectance spectra for the $Na_2Zr_{1-x}Tb_xO_3$ ($0 \leq x \leq 0.20$) samples.

As can be seen from Figure 4, the optical absorption intensity corresponding to the O^{2-}–Tb^{4+} CT transition increased with increasing Tb^{4+} concentration. Among the samples with x ranging from 0 to 0.18 (solubility limit), the $Na_2Zr_{0.82}Tb_{0.18}O_3$ (x = 0.18) sample showed the highest absorption intensity.

3.3. Color Properties

The $L^*a^*b^*Ch^\circ$ color parameters of the $Na_2Zr_{1-x}Tb_xO_3$ ($0 \leq x \leq 0.20$) samples and commercially available yellow $BiVO_4$ (Dainichiseika Color & Chemicals Mfg., Tokyo, Japan), $PbCrO_4$ (NIC, Osaka, Japan) and $ZrSiO_4$:Pr (Kawamura Chemical, Yokkaichishi, Japan) pigments are summarized in Table 1. The photographs are also displayed in Figure 5. The host Na_2ZrO_3 sample had a high L^* value (brightness), and both a^* (redness) and b^* (yellowness) values were almost equal to zero. This sample exhibited a white color.

Table 1. Color coordinate data of the $Na_2Zr_{1-x}Tb_xO_3$ ($0 \leq x \leq 0.20$) samples and the commercially available yellow $BiVO_4$, $PbCrO_4$, and $ZrSiO_4$:Pr pigments.

Sample	L^*	a^*	b^*	C	h°
Na_2ZrO_3	98.0	−0.14	+0.62	0.64	103
$Na_2Zr_{0.95}Tb_{0.05}O_3$	91.5	−6.95	+50.9	51.4	97.8
$Na_2Zr_{0.90}Tb_{0.10}O_3$	86.4	−3.70	+61.5	61.6	93.4
$Na_2Zr_{0.85}Tb_{0.15}O_3$	82.6	−0.62	+66.1	66.1	90.5
$Na_2Zr_{0.82}Tb_{0.18}O_3$	82.4	−0.17	+67.2	67.2	90.1
$Na_2Zr_{0.80}Tb_{0.20}O_3$	66.2	−1.26	+46.5	46.5	91.6
$BiVO_4$	93.3	−15.7	+80.3	81.8	101
$PbCrO_4$	89.9	+1.12	+96.5	96.5	89.3
$ZrSiO_4$:Pr	83.5	−3.28	+70.3	70.4	92.7

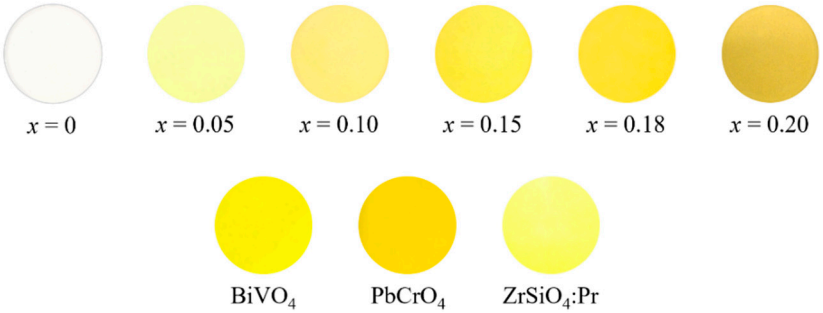

Figure 5. Photographs of the $Na_2Zr_{1-x}Tb_xO_3$ ($0 \leq x \leq 0.20$) samples and the commercial $BiVO_4$, $PbCrO_4$, and $ZrSiO_4$ pigments.

When Zr^{4+} was partially replaced by Tb^{4+}, the b^* value increased dramatically due to the strong absorption of blue light, as shown in Figure 4. In addition, the h° parameter (hue angle) fell into the yellow region of $70 \leq h^\circ \leq 105$. As a result, the Tb^{4+}-doped samples turned yellow. Furthermore, the color of the samples changed from pale to bright yellow as the absorption intensity in the blue light region increased with increasing Tb^{4+} content. Among the samples synthesized in this study, the highest b^* and C (chroma) values were obtained for the $Na_2Zr_{0.82}Tb_{0.18}O_3$ sample, which exhibited the brightest yellow color.

The color coordinate data of the $Na_2Zr_{0.82}Tb_{0.18}O_3$ sample in this study were compared with those of the commercially available yellow pigments, as shown in Table 1 and Figure 5. The yellowness (b^*) of this sample was slightly lower than that of the environmentally friendly $ZrSiO_4$:Pr pigment. However, the h° value of this sample was closer to 90° (pure yellow) than the commercially available $BiVO_4$ and $ZrSiO_4$:Pr pigments. Because the standard deviations of all values for the $L^*a^*b^*Ch^\circ$ color coordinate data were less than 0.1, there was a significance difference between the $Na_2Zr_{0.82}Tb_{0.18}O_3$ pigment and the commercial ones, and we concluded this pigment had a purer yellow color than them.

3.4. Chemical Stability Test

The chemical stability of the $Na_2Zr_{0.82}Tb_{0.18}O_3$ sample was evaluated using the powder sample. The powder samples were soaked in deionized water, 4% CH_3COOH, and 4% NH_4HCO_3 aqueous solutions. The samples were left at room temperature for 5 h

(for deionized water) and 2 h (for acid and base) and then washed with deionized water and ethanol. The samples were then dried at room temperature. The color coordinate data of the samples after the chemical stability tests are summarized in Table 2, and their photographs are also displayed in Figure 6. Unfortunately, the chemical stability of the $Na_2Zr_{0.82}Tb_{0.18}O_3$ sample was insufficient, and each treatment resulted in degradation of the color tone. Therefore, surface coating with a stable compound such as silica is considered necessary for the application of this sample to inorganic pigments. Silica is considered suitable as a coating material because it is a cost-effective, stable, and green compound. If the pigment in this study was coated with silica, we expect it would be a more environmentally friendly yellow pigment than uncoated pigments.

Table 2. Color coordinate data of the $Na_2Zr_{0.82}Tb_{0.18}O_3$ sample before and after the chemical stability test.

Treatment	*L**	*a**	*b**	*C*	*h*°
As synthesized	82.4	−0.17	+67.2	67.2	90.1
Water	62.1	+17.2	+60.4	62.8	74.1
4% CH_3COOH	63.1	+15.8	+65.6	67.5	76.5
4% NH_4HCO_3	63.5	+16.1	+61.1	63.2	75.2

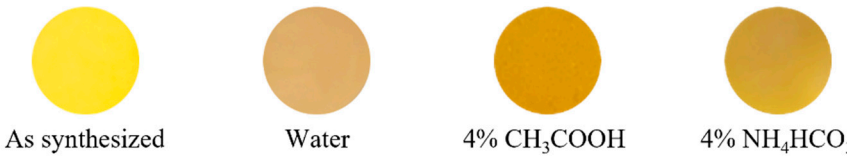

Figure 6. Photographs of the $Na_2Zr_{0.82}Tb_{0.18}O_3$ sample before and after the chemical stability test.

4. Conclusions

Tb^{4+}-doped sodium zirconate samples, $Na_2Zr_{1-x}Tb_xO_3$, were synthesized as environmentally benign inorganic yellow pigments by a solid-state reaction method. In the x range from 0 to 0.18, the samples were obtained in a single-phase form and the lattice volume increased linearly. These results indicate that the solid solutions were successfully obtained in this x region. The Tb^{4+}-doped samples exhibited optical absorption in the blue light region due to the charge transfer transition between O^{2-} and Tb^{4+}. The intensity of this optical absorption increased with increasing Tb^{4+} content. As a result, the color of the samples changed from pale to bright yellow. Among the samples synthesized, the $Na_2Zr_{0.82}Tb_{0.18}O_3$ sample showed the highest yellowness. The yellowness of this sample was inferior to those of commercially available yellow pigments. However, the yellow color purity of this sample was better than those of the existing environmentally friendly types. In addition, no toxic solvents or gases are required or generated in the synthesis of this pigment. Therefore, although the chemical stability of the present sample is not sufficient, it may become a new environmentally friendly inorganic yellow pigment by coating with a stable compound.

Author Contributions: Conceptualization, R.O. and T.M.; methodology, R.O., T.N. and T.M.; validation, R.O. and T.M.; investigation, R.O. and T.N.; data curation, R.O. and T.N.; writing—original draft preparation, R.O.; writing—review and editing, T.M.; supervision, T.M.; funding acquisition, T.M. All authors have read and agreed to the published version of the manuscript.

Funding: This research was funded by JSPS KAKENHI, grant numbers JP22K04698 and JP20H02439.

Institutional Review Board Statement: Not applicable.

Informed Consent Statement: Not applicable.

Data Availability Statement: Data are contained within the article.

Conflicts of Interest: The authors declare no conflict of interest.

References

1. Faulkner, E.B.; Schwartz, R.J. *High Performance Pigments*, 2nd ed.; Wiley-VCH: Weinheim, Germany, 2009.
2. Thara, T.R.A.; Rao, P.P.; Raj, A.K.V.; Sreena, T.S. New series of brilliant yellow colorants in rare earth doped scheelite type oxides, $(LiRE)_{1/2}WO_4$- $BiVO_4$ for cool roof applications. *Sol. Energy Mater. Sol. Cells* **2019**, *200*, 110015. [CrossRef]
3. Kumari, L.S.; Rao, P.P.; Radhakrishnan, A.N.P.; James, V. Brilliant yellow color and enhanced NIR reflectance of monoclinic $BiVO_4$ through distortion in VO_4^{3-} tetrahedra. *Sol. Energy Mater. Sol. Cells* **2013**, *112*, 134–143. [CrossRef]
4. Wendusu; Honda, T.; Masui, T.; Imanaka, N. Novel environmentally friendly (Bi, Ca, Zn, La)VO_4 inorganic yellow pigments. *RSC Adv.* **2013**, *3*, 24941–24945. [CrossRef]
5. Šulcová, P.; Trojan, M. Thermal synthesis and properties of the $(Bi_2O_3)_{1-x}(Ho_2O_3)_x$ pigments. *J. Therm. Anal. Calorim.* **2006**, *83*, 557–559. [CrossRef]
6. Laguna, M.; Núñez, N.O.; Fernández, M.; Ocaña, M. Synthesis and optical properties of environmentally benign and highly uniform $NaCe(MoO_4)_2$ based yellow nanopigments. *J. Alloys Compd.* **2018**, *739*, 542–548. [CrossRef]
7. Nero, G.D.; Cappelletti, G.; Ardizzone, S.; Fermo, P.; Gilardoni, S. Yellow Pr-zircon pigments: The role of praseodymium and of the mineralizer. *J. Eur. Ceram. Soc.* **2004**, *24*, 3603–3611. [CrossRef]
8. Guo, D.; Yang, Q.; Chen, P.; Chu, Y.; Zhang, Y.; Rao, P. The influence of micronization on the properties of Pr-$ZrSiO_4$ pigment. *Dyes Pigm.* **2018**, *153*, 74–83. [CrossRef]
9. Sumaletha, N.; Rajesh, K.; Mukundan, P.; Warrier, K.G.K. Environmentally benign sol–gel derived nanocrystalline rod shaped calcium doped cerium phosphate yellow-green pigment. *J. Sol-Gel Sci. Technol.* **2009**, *52*, 242–250. [CrossRef]
10. Sameera, S.F.; Rao, P.P.; Kumari, L.S.; Koshy, P. New scheelite-based environmentally friendly yellow pigments: $(BiV)_x(CaW)_{1-x}O_4$. *Chem. Lett.* **2009**, *38*, 1088–1089. [CrossRef]
11. Calatayud, J.M.; Alarcón, J. V-containing ZrO_2 inorganic yellow nano-pigments prepared by hydrothermal approach. *Dyes Pigm.* **2017**, *146*, 178–188. [CrossRef]
12. Gorodylova, N.; Šulcová, P. Polymerizable precursor method vs solid state reaction for the synthesis of $Ni_3(PO_4)_2$ yellow hue pigment with advanced characteristics. *J. Alloys Compd.* **2022**, *903*, 163854. [CrossRef]
13. Zhou, W.; Ye, J.; Liu, Z.; Wang, L.; Chen, L.; Zhuo, S.; Liu, Y.; Chen, W. High near-infrared reflective $Zn_{1-x}A_xWO_4$ pigments with various hues facilely fabricated by tuning doped transition metal ions (A = Co, Mn, and Fe). *Inorg. Chem.* **2022**, *61*, 693–699. [CrossRef] [PubMed]
14. Pettini, F.; Seguelong, T.; Inventors; Chimie, R.; Assignee. Pigmented substrates comprising terbium compound colorants. U.S. Patent 5688316, 18th November 1997.
15. Mesíková, Ž.; Šulcová, P.; Trojan, M. Synthesis and description of $SrSn_{0.6}Ln_{0.4}O_3$ perovskite pigments. *J. Therm. Anal. Calorim.* **2008**, *91*, 163–166. [CrossRef]
16. Lunáková, P.; Trojan, M.; Luxová, J.; Trojan, J. $BaSn_{1-x}Tb_xO_3$: A new yellow pigment based on a perovskite structure. *Dyes Pigm.* **2013**, *96*, 264–268. [CrossRef]
17. Oka, R.; Tsukimori, T.; Inoue, H.; Mausi, T. Perovskite-type $ALnO_3$ (*A* = Ca, Sr, Ba; *Ln* = Ce, Pr, Tb) oxides as environmentally friendly yellow pigments. *J. Ceram. Soc. Jpn.* **2017**, *125*, 652–656. [CrossRef]
18. Raj, A.K.V.; Rao, P.P.; Sameera, S.; James, V.; Divya, S. Synthesis of novel nontoxic yellow pigments: $Sr_2Ce_{1-x}Tb_xO_4$. *Chem. Lett.* **2014**, *43*, 985–987. [CrossRef]
19. Raj, A.K.V.; Rao, P.P.; Divya, S.; Ajuthara, T.R. Terbium doped Sr_2MO_4 [M = Sn and Zr] yellow pigments with high infrared reflectance for energy saving applications. *Powder Technol.* **2017**, *311*, 52–58. [CrossRef]
20. Raj, A.K.V.; Rao, P.P.; Sreena, T.S. Color tunable pigments with high NIR reflectance in terbium-doped cerate systems for sustainable energy saving applications. *ACS Sustain. Chem. Eng.* **2019**, *7*, 8804–8815. [CrossRef]
21. Chen, J.; Xie, W.; Guo, X.; Huang, B.; Xiao, Y.; Sun, X. Near infrared reflective pigments based on Bi_3YO_6 for heat insulation. *Ceram. Int.* **2020**, *46*, 24575–24584. [CrossRef]
22. Bastow, T.J.; Hobday, M.E.; Smith, M.E.; Whitfield, H.J. Structural characterisation of Na_2ZrO_3. *Solid State Nucl. Magn. Reson.* **1994**, *3*, 49–57. [CrossRef]
23. Alcántar-Vázquez, B.; Diaz, C.; Romero-Ibarra, I.C.; Lima, E.; Pfeiffer, H. Structural and CO_2 chemisorption analyses on $Na_2(Zr_{1-x}Al_x)O_3$ solid solutions. *J. Phys. Chem. C* **2013**, *117*, 16483–16491. [CrossRef]
24. Song, S.; Kotobuki, M.; Zheng, F.; Xu, C.; Hu, N.; Lu, L.; Wang, Y.; Li, W.-D. Y-doped Na_2ZrO_3: A Na-rich layered oxide as a high-capacity cathode material for sodium-ion batteries. *ACS Sustain. Chem. Eng.* **2017**, *5*, 4785–4792. [CrossRef]
25. Duan, Y.; Lekse, J.; Wang, X.; Li, B.; Alcántar-Vázquez, B.; Pfeiffer, H.; Halley, J.W. Electronic structure, phonon dynamical properties, and CO_2 capture capability of $Na_{2-x}M_xZrO_3$ (*M* = Li,K): Density-functional calculations and experimental validations. *Phys. Rev. Appl.* **2015**, *3*, 044013. [CrossRef]
26. Shannon, R.D. Revised effective ionic radii and systematic studies of interatomic distances in halides and chalcogenides. *Acta Crystallogr. Sect. A Found. Adv.* **1976**, *32*, 751–767. [CrossRef]
27. Verma, R.K.; Kumar, K.; Rai, S.B. Inter-conversion of Tb^{3+} and Tb^{4+} states and its fluorescence properties in MO–Al_2O_3: Tb (M = Mg, Ca, Sr, Ba) phosphor materials. *Solid State Sci.* **2010**, *12*, 1146–1151. [CrossRef]